Insights into the acylation mechanism of class A β-lactamases from molecular dynamics simulations of the TEM-1 enzyme complexed with benzylpenicillin

ARTICLE *in* JOURNAL OF THE AMERICAN CHEMICAL SOCIETY · FEBRUARY 2003

Impact Factor: 12.11 · DOI: 10.1021/ja027704o · Source: PubMed

4 AUTHORS, INCLUDING:

Kenneth M Merz
Michigan State University
273 PUBLICATIONS **23,670** CITATIONS

SEE PROFILE

J|A|C|S
ARTICLES
Published on Web 12/24/2002

Insights into the Acylation Mechanism of Class A β-Lactamases from Molecular Dynamics Simulations of the TEM-1 Enzyme Complexed with Benzylpenicillin

Natalia Díaz,[†,§] Tomás L. Sordo,[†] Kenneth M. Merz Jr.,*[,‡] and Dimas Suárez*[,†]

Contribution from the Departamento de Química Física y Analítica, Universidad de Oviedo, C/ Julián Clavería 8, 33006 Oviedo, Spain, and Department of Chemistry, The Pennsylvania State University, 152 Davey Laboratory, University Park, Pennsylvania 16802-6300 USA

Received July 15, 2002; E-mail: dimas@correo.uniovi.es

Abstract: Herein, we present results from molecular dynamics MD simulations (~1 ns) of the TEM-1 β-lactamase in aqueous solution. Both the free form of the enzyme and its complex with benzylpenicillin were studied. During the simulation of the free enzyme, the conformation of the Ω loop and the interresidue contacts defining the complex H-bond network in the active site were quite stable. Most interestingly, the water molecule connecting Glu166 and Ser70 does not exchange with bulk solvent, emphasizing its structural and catalytic relevance. In the presence of the substrate, Ser130, Ser235, and Arg244 directly interact with the β-lactam carboxylate via H-bonds, whereas the Lys234 ammonium group has only an electrostatic influence. These interactions together with other specific contacts result in a very short distance (~3 Å) between the attacking hydroxyl group of Ser70 and the β-lactam ring carbonyl group, which is a favorable orientation for nucleophilic attack. Our simulations also gave insight into the possible pathways for proton abstraction from the Ser70 hydroxyl group. We propose that either the Glu166 carboxylate-Wat1 or the substrate carboxylate-Ser130 moieties could abstract a proton from the nucleophilic Ser70.

Introduction

The most important mechanism through which bacteria have become resistant to β-lactam activity is the production of hydrolytic enzymes known as β-lactamases.[1,2] The mechanistic division of β-lactamases is into the serine enzymes, in which the essential serine is acylated by the β-lactam substrates, and into the zinc metallo-enzymes, where the zinc ion(s) in the active site efficiently catalyze the hydrolysis of a broad spectrum of β-lactam antibiotics.[3] For historical reasons, the most usual classification of these enzymes is based on the comparison of their amino acid sequences. This separates the serine β-lactamases into three classes A, C, and D, whereas the zinc-β-lactamases are grouped together into the structurally and kinetically heterogeneous class B.

The serine β-lactamases outnumber the zinc-enzymes and are considered a more immediate threat.[4] Their catalytic action is characterized by a simple acylenzyme pathway.[5] In the first step, after establishing the Michaelis complex, β-lactams react with serine β-lactamases to give an acylenzyme intermediate. In a second step, the intermediate is hydrolyzed by a water molecule in order to regenerate the active site for the next turnover. Among the serine enzymes, the class A enzymes constitute the majority of penicillin destroying enzymes and, therefore, have been intensively studied by means of high-resolution X-ray crystallography, enzyme kinetics, site-directed mutagenesis experiments, and molecular simulations.[6] On the basis of this large amount of data, the active-site residues which have been found to play an important role in the mechanism of all the class-A β-lactamases are the following: the nucleophilic residue Ser70, several conserved residues as Lys73, Lys234, Glu166 and Ser130, and a water molecule (Wat1) bridging the Glu166 carboxylate with Ser70 (the sequence numbering of Ambler et al. is used[7]). In addition, the side chains and/or backbone atoms of other residues (Asn170, Ala237, Ser235, Arg244, etc.) stabilize the acylenzyme intermediate. In particular, the main-chain N atoms of Ser70 and Ala237 form the so-called "oxyanion hole" which interacts with the oxygen of the β-lactam carbonyl group.

General base catalysis is thought to increase the nucleophilicity of Ser70 in the acylation step of the catalytic process. Similarly, the hydrolytic water is supposed to be deprotonated by a basic residue prior to the rupture of the acylenzyme intermediate. For the hydrolytic step, there exists a consensus that the conserved residue in the class A β-lactamase, Glu166,

* To whom correspondence should be addressed. Fax: +34-985103125.
† Departamento de Química Física y Analítica, Universidad de Oviedo.
‡ Department of Chemistry, The Pennsylvania State University.
§ Current address: Laboratoire de Dynamique Moleculaire, Institut Jean-Pierre Ebel, 41 rue Jules Horowitz, 38027 Grenoble, France.

(1) Walsh, C. *Nature* **2000**, *406*, 775−781.
(2) Wright, G. D. *Chem. Biol.* **2000**, *7*, 127−132.
(3) Waley, S. G. *β-Lactamases: Mechanism of Action*; Page, M. I., Ed.; Blackie Academic & Professional: London, 1992; pp 199−227.
(4) Maiti, S. N.; Philips, O. A.; Micetich, R. G.; Livermore, D. M. *Curr. Med. Chem.* **1998**, *5*, 441−456.
(5) Page, M. I. *Chem. Commun.* **1998**, 1609−1617.
(6) Matagne, A.; Lamotte-Brasseur, J.; Frère, J. M. *Biochem. J.* **1998**, *330*, 581−598.
(7) Ambler, R. P.; Coulson, A. F.; Frére, J. M.; Ghuysen, J. M.; Jaurin, B.; Joris, B.; Levesque, R.; Tiraby, G.; Waley, S. G. *Biochem. J.* **1991**, *276*, 269−272.

10.1021/ja027704o CCC: $25.00

activates Wat1 for attack on the carbonyl carbon.[6] For the mechanism of acylation, a less widely accepted hypothesis suggests that the carboxylate of Glu166 accepts a proton from Ser70 either directly or mediated by Wat1.[8,9] This proton can then be delivered to the leaving nitrogen atom through a network of hydrogen bonds involving Lys73 and the hydroxyl group of Ser130. Very recently, this proposal has gained support thanks to an ultrahigh-resolution structure (0.85 Å) of the TEM-1 β-lactamase in which a boronic acid inhibitor is covalently bound to the Oγ of Ser70, whereas Glu166 is clearly protonated.[10]

The mechanistic proposal for the acylation process in which Glu166 acts as a base catalyst remains controversial. This is well illustrated by site-directed mutagenesis experiments performed on Glu166.[11,12] Thus, the replacement of the negatively charged Glu166 by a neutral asparagine in the TEM-1 enzyme yields mutant enzymes forming *stable* acylenzymes whose structure has been determined by X-ray crystallography.[11] Careful analyses of the kinetic properties of the native and mutant forms of the TEM-1 enzyme reacting with different substrates show that the Glu166Asn mutation decreases by $\sim 10^9$ factor the kinetic constant for the deacylation step.[12] This large impact from the mutation of Glu166 is in agreement with its role as a basic catalyst during the hydrolysis of the acylenzyme intermediate. On the other hand, the acylation rate constants (k_{acyl}/K_M) were also affected, their values being decreased by 2 orders of magnitude with respect to those of the wild-type enzyme. However, the observed acylation rates with the Glu166Asn mutant of the TEM-1 enzyme were of the same order of magnitude as those measured with other penicillin-recognizing proteins (PRPs) which lack any residue analogous to Glu166.[13] Overall, these results confirm that Glu166 is crucial for the deacylation process and has a nonnegligible effect on the acylation of the TEM-1 enzyme. However, it is also clear that these experimental data do not supply a definitive picture for the precise role of Glu166 during the acylation process.

Regardless, the exact role of Glu166 in the acylation step, the *catalytic* acylation of the Glu166Asn mutant enzymes must rely on an alternative mechanism without the direct participation of Glu166. In fact, the same mechanism could occur in both the wild-type and mutant enzymes. Therefore, other proposals assign an active kinetic role to Lys73 or Ser130, which are strictly conserved residues in the class A β-lactamases. Herein, we briefly comment on two particular mechanisms. It has been proposed that the ϵ-amino group of Lys73, which has a close contact with Ser70 in the Glu166Asn acylenzyme crystal structure, is neutral due to the active site environment.[11] Alternatively, a substrate-induced mechanism has been proposed in which the pK_a of Lys73 is reduced upon substrate binding.[14] Thus, a neutral Lys73 residue could act as a general base catalyzing the acylation step, whereas the hydroxyl group of Ser130 could participate in the proton transfer to the β-lactam N atom. However, continuum electrostatic calculations in the absence and presence of different types of β-lactam antibiotics have assigned the pK_a for Lys73 above 10,[15,16] which is in agreement with experimental pK_a determinations.[17] These results are clearly inconsistent with an unprotonated Lys73 acting as the general base. On the other hand, several molecular modeling studies,[18−20] have shown that the β-lactam carboxylate and the Ser130 hydroxyl group may assist both the activation of Ser70 and the protonation of the leaving β-lactam N atom in penicillins. On the basis of quantum chemical calculations on the entire enzyme-benzylpenicillin complex, we recently characterized catalytic pathways for the Ser130 and carboxylate assisted routes which were compatible with the experimental kinetics of the TEM-1 enzyme.[20]

The viability of one catalytic pathway or another largely depends on factors that are not entirely clear: the mobility of the active-site residues, the location of the catalytic water molecules, the actual protonation state of the Glu166···Lys73 pair, etc.. In this respect, molecular dynamics (MD) simulations constitute a valuable tool that is capable of determining the nature and stability of contacts between functional groups that are essential elements in the proposed reaction mechanisms. To our knowledge, the only MD study of the unbound form of a fully solvated class A β-lactamase is a short trajectory (180 ps) of the PC1 enzyme from *Streptomyces aureus*.[8] In this latter article, the authors speculated that an acylation mechanism in which the Glu166 carboxylate acts as a base catalyst, could be dynamically feasible since the large mobility of the Glu166 residue during their MD simulation resulted in a close contact (2.5−3.0 Å) with the Ser70 hydroxyl group. Recently, MD simulations were carried out on the wild-type and the Met69Leu mutant of the TEM-1 enzyme complexed with clavunalate, a typical inhibitor of serine β-lactamases.[21] However, the structural and energetic analyses reported were limited to what was necessary in order to analyze the subtle global effects of the Met69Leu mutation which confers the observed inhibitor-resistance to the enzyme. On the other hand, substrate binding to class A β-lactamases, has been studied using molecular mechanics methodologies.[9,16,18,22,23] It must be noted, however, that energy minimization methodologies are not as effective as MD approaches in understanding the nature of intra-protein and protein−substrate interactions.

In this article, we explored the likely conformations of the TEM-1 β-lactamase by computing long MD trajectories (∼1.2 ns) for the fully solvated enzyme both in its free form (**TEM1** simulation) and in its complexed form with benzylpenicillin as

(8) Vijayakumar, S.; Ravishanker, G.; Pratt, R. F.; Beveridge, D. L. *J. Am. Chem. Soc.* **1995**, *117*, 1722−1730.
(9) Lamotte-Brasseur, J.; Jacob-Dubuisson, F.; Dive, G.; Frère, J. M.; Ghuysen, J. M. *Biochem. J.* **1992**, *282*, 189−195.
(10) Minasov, G.; Wang, X.; Shoichet, B. K. *J. Am. Chem. Soc.* **2002**, *124*, 5333−5340.
(11) Strydnadka, N. C. J.; Adachi, H.; Jensen, S. E.; Johns, K.; Sielecki, A.; Betzel, C.; Sutoh, K.; James, M. N. J. *Nature* **1992**, *359*, 700−705.
(12) Gillaume, G.; Vanhove, M.; Lamotte-Brasseur, J.; Ledent, P.; Jamin, M.; Joris, B.; Frére, J. M. *J. Biol. Chem.* **1997**, *272*, 5438−5444.
(13) Massova, I.; Mobashery, S. *Antimicrob. Agents. Chemother.* **1998**, *42*, 1−17.
(14) Zawadzke, L. E.; Chen, C. C. H.; Banerjee, S.; Li, Z.; Wäsch, S.; Kapadia, G.; Moult, J.; Herzberg, O. *Biochemistry* **1996**, *35*, 16 475−16 482.
(15) Raquet, X.; Lounnas, V.; Lamotte-Brasseur, J.; Frère, J. M.; Wade, R. C. *Biophys. J.* **1997**, *73*, 2416−2426.
(16) Lamotte-Brasseur, J.; Lounnas, V.; Raquet, X.; Wade, R. C. *Protein Sci.* **1999**, *8*, 404−409.
(17) Damblon, C.; Raquet, X.; Lian, L. Y.; Lamotte-Brasseur, J.; Fonzé, E.; Charlier, P.; Roberts, G. C. K.; Frére, J. M. *Proc. Natl. Acad. Sci. USA* **1996**, *93*, 1747−1752.
(18) Ishiguro, M.; Imajo, S. *J. Med. Chem.* **1996**, *39*, 2207−2218.
(19) Atanasov, B.; Mustafi, D.; Makinen, M. W. *Proc. Nat. Acad. Sci* **2000**, *97*, 3160−3165.
(20) Díaz, N.; Suárez, D.; Sordo, T. L.; Merz, K. M., Jr. *J. Phys. Chem. B* **2001**, *105*, 11 302−11 313.
(21) Meroueh, S. O.; Roblin, P.; Golemi, D.; Maveyraud, L.; Vakulenko, S. B.; Zhang, Y.; Samama, J.-P.; Mobashery, S. *J. Am. Chem. Soc.* **2002**, *124*, 9422−9430.
(22) Matagne, A.; Lamotte-Brasseur, J.; Dive, G.; Knox, J. R.; Frère, J. M. *Biochem. J.* **1993**, *293*, 607−611.
(23) Lamotte-Brasseur, J.; Dive, G.; Dideberg, O.; Charlier, P.; Frére, J. M.; Ghuysen, J. M. *Biochem. J.* **1991**, *279*, 213−221.

a typical substrate (**TEM1-BP** simulation). In particular, we studied the protonation state of the active site in which the charge of Glu166 is set to −1 and that of Lys73 to +1. Along the simulations, we characterized the interactions between the important functional groups, the structural and dynamical changes upon substrate binding, the specific role of the key residues in anchoring the substrate, etc. For the Michaelis complex between the TEM-1 enzyme and benzylpenicillin, we simulated a second configuration in which both Glu166 and Lys73 were neutral (this simulation is labeled **TEM1-BP-2**). The **TEM1-BP-2** configuration, which might be of the most mechanistic interest, arises from the transfer of a proton from Lys73→Glu166 in the **TEM1-BP** state. The relative stability of the **TEM1-BP** and **TEM1-BP-2** configurations were analyzed by combining semiempirical quantum chemical calculations on enzyme−substrate subsystems and density functional calculations (DFT) on the Glu166-Lys73 side chains. All of these theoretical results have provided further insights into the catalytic processes taking place in the active site of class A β-lactamases.

Methods

MD Simulation of the Unbound Form of the TEM-1 Enzyme. Starting coordinates for the protein atoms and the crystallographic water molecules were taken from the solid-state structure of the TEM-1 β-lactamase at 1.8 Å resolution (PDB ID code: 1BLT).[24] This high-resolution structure has a sulfate anion in the active site that was deleted from the coordinate file. The protonation state for the ionizable residues were set to their normal ionization state at pH 7, except Asp214 which is neutral in the TEM-1 active site.[15,24] To generate the **TEM1** model, the protein atoms, as well as the water molecules of the crystal structure, were surrounded by a periodic box of TIP3P water molecules that extended 10 Å from the protein atoms. Na^+ counterions were placed by the LEaP program[25] 7 Å beyond the Oγ@Ser70 atom to neutralize the −6 charge of the **TEM1** model. This resulted in the **TEM1** system with 4080 protein atoms being solvated by 199 X-ray water molecules and 9491 additional water molecules. The parm96 version of the all-atom AMBER force field was used to model the system.[26]

To remove bad contacts in the initial geometry, energy minimization was done using conjugate-gradient minimization (2500 steps for the water molecules followed by 2500 steps for the entire system). MD simulations were carried out using SANDER included in version 5.0 of the AMBER suite of programs.[27] The time step was chosen to be 1.5 fs and the SHAKE algorithm[28] was used to constrain all bonds involving hydrogen atoms. A nonbond pairlist cutoff of 9.0 Å was used and the nonbonded pairlist was updated every 25 time steps.[29] The pressure (1 atm) and the temperature (300 K) of the system were controlled during the MD simulations by Berendsen's method[30] (separate scaling factors for the solute and the solvent temperatures were used). Periodic boundary conditions were applied to simulate a continuous system.[29] To include the contributions of long-range

Scheme 1

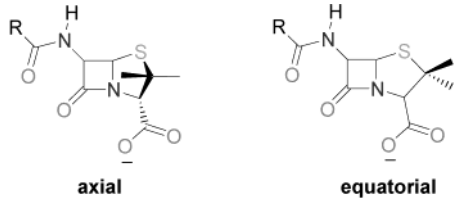

interactions, the Particle−Mesh−Ewald (PME) method[31] was used with a grid size of 64 × 64 × 64 (grid spacing of ~1 Å) combined with a fourth-order B-spline interpolation to compute the potential and forces in between grid points. The estimated root-mean-squared deviations of the PME force errors[32] during the simulations were lower than 10^{-4}.

For the **TEM1** model, an equilibration period of 200 ps resulted in a stable trajectory, as evidenced by the convergence of the dimensions of the simulation box and the evolution of the total energy of the system. Subsequently, a 1 ns trajectory was computed and coordinates were saved for analysis every 50 time steps. All of the MD results were analyzed using the CARNAL module of AMBER 5.0 and some other specific trajectory analysis software developed locally. In these analyses, the following criteria were employed to discriminate between *short* and *long* (and presumably weaker) hydrogen bond interactions. We assign hydrogen bonds as *short* and stable when the average distances of the O/N···O interaction is less than 3.0 Å and the percent occurrence is on the order of 100%. Other polar contacts, with average O/N···O distances within 3.0−3.5 Å and a percent occurrence that is less than 100%, are assigned as *long* and weak hydrogen bond interactions. Structural figures were produced with the programs Molscript[33] and Raster3D.[34]

Parametrization of Benzylpenicillin. The five-membered thiazolidine ring of benzylpenicillin can exist in two conformations,[35] the axially oriented carboxylate group and the equatorially disposed conformer (see Scheme 1). According to NMR experiments, ring flipping of the thiazolidine moiety occurs quite freely in solution.[36,37] However, it is commonly thought that the equatorial conformation is biologically active whereas the axial conformation is inactive.[38] In fact, the thiazolidine ring shows an equatorial conformation in all of the crystal structures of acyl-enzymes derived from penicillins.[11,39−42] Nevertheless, others contend that it is still unclear which is the biologically active conformer that binds to penicillin recognizing proteins.[43]

We carried out HF/6-31G* optimizations in the gas-phase for the two conformers of benzylpenicillin (BP) which differed in the ring puckering of the thiazolidine moiety using the Gaussian 98 suite of programs.[44] Single-point MP2/6-31+G** calculations on the HF/6-31G* geometries predict that the axial conformer is the more stable structure by 2.5 kcal/mol. To derive the corresponding force-field parameters for BP which are not present in the standard AMBER

(24) Jelsch, C.; Mourey, L.; Masson, J. M.; Samama, J. P. *Proteins: Struct. Func. Genet.* **1993**, *16*, 364−383.
(25) Schafmeister, C.; Ross, W. S.; Romanovski, V. *LEap*, 1.0 ed.; University of California: San Francisco, 1995.
(26) Cornell, W. D.; Cieplak, P.; Bayly, C. I.; Gould, I. R.; Merz, K. M., Jr.; Ferguson, D. M.; Spellmeyer, D. C.; Fox, T.; Caldwell, J. W.; Kollman, P. A. *J. Am. Chem. Soc.* **1995**, *117*, 5179−5197.
(27) Case, D. A.; Pearlman, D. A.; Caldwell, J. W.; Cheatham II, T. E.; Ross, W. S.; Simmerling, C. L.; Darden, T. A.; Merz, K. M., Jr.; Stanton, R. V.; Cheng, A. L.; Vincent, J. J.; Crowley, M.; Ferguson, D. M.; Radmer, R. J.; Seibel, G. L.; Singh, U. C.; Weiner, P. K.; Kollman, P. A. *AMBER*, 5.0 ed.; University of California: San Francisco, 1997.
(28) van Gunsteren, W. F.; Berendsen, H. J. C. *Mol. Phys.* **1977**, *34*, 1311.
(29) Allen, M. P.; Tildesley, D. J. *Computer Simulation of Liquids*; Clarendon Press: Oxford, 1987.
(30) Berendsen, H. J. C.; Potsma, J. P. M.; van Gunsteren, W. F.; DiNola, A. D.; Haak, J. R. *J. Chem. Phys.* **1984**, *81*, 3684−3690.
(31) Essman, V.; Perera, L.; Berkowitz, M. L.; Darden, T.; Lee, H.; Pedersen, L. G. *J. Chem. Phys.* **1995**, *103*, 8577−8593.
(32) Petersen, H. G. *J. Chem. Phys.* **1995**, *103*, 3668−3679.
(33) Kraulis, P. J. *J. Appl. Crystallogr.* **1991**, *24*, 946−950.
(34) Merritt, E. A.; Bacon, D. J. *Methods Enzymol.* **1997**, *277*, 505−524.
(35) Boyd, D. B. In *Chemistry and Biology of β-Lactam Antibiotics*; Morin, R. B., Gorman, M., Eds.; Academic Press: London, 1982; Vol. 1, pp 437−439.
(36) Clayden, N. J.; Dobson, C. M.; Lian, L.-Y.; Twyman, J. M. *J. Chem. Soc., Perkin Trans. II* **1986**, 1933−1940.
(37) Twyman, J. M.; Fattah, J.; Dobson, C. M. *J. Chem. Soc., Chem. Commun.* **1991**, 647−649.
(38) Keith, D. D.; Tengi, J.; Rossman, P.; Todaro, L.; Weigele, M. *Tetrahedron* **1983**, *39*, 2445−2458.
(39) Jhoti, H.; Singh, O. M.; Weir, M. P.; Cooke, R.; Murray-Rust, P.; Wonacott, A. *Biochemistry* **1994**, *33*, 8417−8427.
(40) Miyashita, K.; Massova, I.; Taibi, P.; Mobashery, S. *J. Am. Chem. Soc.* **1995**, *117*, 11 055−11 059.
(41) Maveyraud, L.; Massova, I.; Birck, C.; Miyashita, K.; Samama, J. P.; Mobashery, S. *J. Am. Chem. Soc.* **1996**, *118*, 7435−7440.
(42) Chen, C. C. H.; Herzberg, O. *Biochemistry* **2001**, *40*, 2351−2358.
(43) Nangia, A.; Desiraju, G. R. *J. Mol. Struct.* **1999**, *474*, 65−79.

database, we followed the procedure suggested by Fox et al.[45] to be consistent with the AMBER force field.[26] For each of the BP conformers, we computed the electrostatically derived atomic charges using the RESP methodology.[46] The use of RESP charges ensures that electrostatic interactions between all atoms of the enzyme/small molecule complex were treated on an equal basis. Some structural data required to represent the equilibrium geometry of the bicyclic skeleton of benzylpenicillin were extracted from the HF/6-31G* optimized structures. Most of the bond, angle, and dihedral parameters were available from the AMBER force field. The missing parameters were assigned the values of similar types found in the force field. The van der Waals (vdW) parameters were taken from the closest existing AMBER atom types according to the electronic structure similarity. In addition, some specific torsion parameters were adjusted to reproduce the MP2/6-31+G**//HF/6-31G* ΔE between the equatorial and axial conformers.

The BP parametrization was tested by minimizing *in vacuo* the geometry of the two conformers, their resultant structures were very similar to the HF/6-31G* ones. For example, root-mean-square deviation of the heavy atoms in the bicyclic nucleus between the AMBER and the HF/6-31G* structures is 0.26 and 0.13 Å for the equatorial and axial conformers, respectively. The molecular mechanics (MM) energy of the axial structure is 2.7 kcal/mol below that of the equatorial structure in close agreement with the MP2/6-31+G**//HF/6-31G* calculations. To further test our BP parametrization, we computed a 1.0 ns MD trajectory of BP fully solvated in a periodic box of 3885 TIP3P waters. During the simulation, we observed several flips of the thiazolidine ring between the equatorial and axial conformers. The final BP parameters are given in the Supporting Information.

MD Simulations of the Michaelis Complex Formed between the TEM-1 Enzyme and Benzylpenicillin. The starting structure for the **TEM1-BP** and **TEM1-BP-2** models was a Michaelis complex between the TEM-1 enzyme and benzylpenicillin described previously.[20] This Michaelis complex was initially constructed from the 1BLT X-ray coordinates. The structure of the active site was relaxed by means of a short MD trajectory (100 ps) in which only residues and water molecules within 15 Å of the Oγ@Ser70 atom were allowed to move. The benzylpenicillin substrate was then accommodated in the active site by molecular modeling and partial relaxation through energy-minimization using a QM/MM hybrid Hamiltonian (further details are given elsewhere).[20]

The water molecules in the QM/MM structure were retained and placed in the **TEM1-BP** and **TEM1-BP-2** systems. For the **TEM1-BP-2** model, the Glu166 carboxylate and the Lys73 ammonium group were converted into neutral carboxyl and amino groups, respectively. The resultant enzyme−substrate systems were surrounded by a periodic box of solvent molecules, which contained a total of 9664 water molecules. Seven Na^+ counterions were placed by LEaP to neutralize the models, which were then minimized for 2500 steps using the parm96 version of the AMBER force field. The MD simulation protocols for **TEM1-BP** and **TEM1-BP-2** were identical to those for the unbound model (**TEM1**).

Energetic Analysis. For the **TEM1-BP** and **TEM1-BP-2** simulations, a series of QM/MM minimizations were performed in which the BP substrate, the Wat1 molecule, and the side chains of Ser70, Ser130, Glu166, Lys73, Lys234, and Arg244 (QM region) were relaxed, whereas the rest of the protein and a solvent cap of 1500 water molecules centered on the Oγ@Ser70 atom (MM region) were held fixed. Initial geometries were taken from snapshots extracted every 20 ps during the simulations. In these calculations, the AM1 Hamiltonian[47] was used to describe the QM region (AM1 is known to provide a better root-mean-square deviation for β-lactam molecules than other semiempirical methods such as MNDO and PM3, when the results were compared with crystallographical data[48−50]). The AMBER force field was used for the rest of the system. Hydrogen link atoms were placed at the corresponding Cβ atoms to cap exposed valence sites due to bonds, which crossed the QM-MM boundary. The ROAR 2.0 program[51] was used to carry out the QM/MM minimizations.

From the QM/MM relaxed structures, we selected subsystems formed by all residues within a distance of 9 Å to Oγ@Ser70 including most of the residues in the Ω loop (residues: 68−76, 103−107, 125−135, 161−174, and 234−248). Terminal *N*-methylamine or acetyl groups were placed at the C and N backbone atoms of those residues cleaved from the protein main chain by the truncation process. In addition, the BP substrate and the Wat1 molecule were also extracted. Single-point AM1 calculations were performed on these subsystems using the Divide and Conquer (D&C) approach.[52] Incorporation of solvent effects within a QM methodology was accomplished by merging the D&C algorithm with the Poisson−Boltzmann (PB) equation.[53] In the PB calculations, the solute was represented by Charge Model 2 (CM2) atomic charges.[54] An additional "nonpolar" contribution due to the creation of a solute cavity in the continuum is accounted for by a term proportional to the solvent accessible surface area of the solute. The DivCon99 program[55] was employed to perform the D&C AM1 calculations using the dual buffer layer scheme (inner buffer layer of 4.0 Å and an outer buffer layer of 2.0 Å) with one protein residue per core. This D&C *subsetting* with a total buffer region of 6.0 Å gives accurate relative energies.[56] A cutoff of 9.0 Å was used for the off-diagonal elements of the Fock, 1-electron and density matrixes.

Solute entropic contributions were estimated for the series of subsystems taken from the trajectories by using the *nmode* module of the AMBER 5.0 package. This program uses the normal modes and standard statistical thermodynamical formulas to estimate entropic contributions. Prior to the normal mode calculations, the geometries of the **TEM1-BP**/**TEM1-BP-2** subsystems described by their AMBER representations were minimized until the root-mean-squared deviation of the elements in the gradient vector was less than 10^{-5} kcal/(mol Å). The ROAR 2.0 program was used to carry out the geometry optimizations driven by a limited memory BFGS minimizer.[57] All minimizations and normal mode calculations were carried out with a distance-dependent dielectric ($\epsilon = 4r$) to mimic solvent screening and with no cutoff for nonbonded interactions. As noted in previous work,[58] this

(44) Frisch, M. J.; Trucks, G. W.; Schlegel, H. B.; Scuseria, G. E.; Robb, M. A.; Cheeseman, J. R.; Zakrzewski, V. G.; Montgomery, J. A.; Stratmann, J., R. E.; Burant, J. C.; Dapprich, S.; Millam, J. M.; Daniels, A. D.; Kudin, K. N.; Strain, M. C.; Farkas, O.; Tomasi, J.; Barone, V.; Cossi, M.; Cammi, R.; Mennucci, B.; Pomelli, C.; Adamo, C.; Clifford, S.; Ochterski, J.; Petersson, G. A.; Ayala, P. Y.; Cui, Q.; Morokuma, K.; Malick, D. K.; Rabuck, A. D.; Raghavachari, K.; Foresman, J. B.; Cioslowski, J.; Ortiz, J. V.; Stefanov, B. B.; Liu, G.; Liashenko, A.; Piskorz, P.; Komaromi, I.; Gomperts, R.; Martin, R. L.; Fox, D. J.; Keith, T.; Al-Laham, M. A.; Peng, C. Y.; Nanayakkara, A.; Gonzalez, C.; Challacombe, M.; Gill, P. M. W.; Johnson, B.; Chen, W.; Wong, M. W.; Andres, J. L.; Gonzalez, C.; Head-Gordon, M.; Replogle, E. S.; Pople, J. A. *Gaussian 98*, revision A.6; Gaussian, Inc.: Pittsburgh, PA, 1998.
(45) Fox, T.; Kollman, P. A. *J. Phys. Chem. B* **1998**, *102*, 8070−8079.
(46) Bayly, C. A.; Cieplak, P.; Cornell, W. D.; Kollman, P. A. *J. Phys. Chem.* **1993**, *97*, 10 269−10 280.
(47) Dewar, M. J. S.; Zoebisch, E. G.; Healy, E. F.; Stewart, J. J. P. *J. Am. Chem. Soc.* **1985**, *107*, 3902−3909.
(48) Taibi-Tronche, P.; Massova, I.; Vakulenko, S. B.; Lerner, S. A.; Mobashery, S. *J. Am. Chem. Soc.* **1996**, *118*, 7441−7448.
(49) Frau, J.; Coll, M.; Donoso, J.; Muñoz, F. *J. Mol. Struct. (THEOCHEM)* **1991**, *231*, 109−124.
(50) Frau, J.; Donoso, J.; Muñoz, F.; García-Blanco, F. *J. Mol. Struct. (THEOCHEM)* **1991**, *251*, 205−218.
(51) Cheng, A.; Stanton, R. S.; Vincent, J. J.; van der Vaart, A.; Damodaran, K. V.; Dixon, S. L.; Hartsough, D. S.; Mori, M.; Best, S. A.; Monard, G.; Garcia, M.; Van Zant, L. C.; Merz, K. M. J. *ROAR 2.0*; The Pennsylvania State University, 1999.
(52) Yang, W.; Lee, T.-S. *J. Chem. Phys.* **1995**, *103*, 5674−5678.
(53) Gogonea, V.; Merz, K. M., Jr. *J. Phys. Chem. A* **1999**, *103*, 5171−5178.
(54) Li, J.; Cramer, C. J.; Truhlar, D. G. *J. Phys. Chem. A* **1998**, *102*, 1820−1831.
(55) Dixon, S. L.; van der Vaart, A.; Gogonea, V.; Vincent, J. J.; Brothers, E. N.; Suárez, D.; Westerhoff, L. M.; Merz, K. M. J. *DIVCON99*; The Pennsylvania State University, 1999.
(56) van der Vaart, A.; Suárez, D.; Merz, K. M., Jr. *J. Chem. Phys.* **2000**, *113*, 10 512−10 523.
(57) Lui, D. C.; Nocedal, J. *Mathematical Programming* **1989**, *45*, 503−528.
(58) Chong, L. T.; Duan, Y.; Wang, L.; Massova, I.; Kollman, P. A. *Proc. Natl. Acad. Sci.* **1999**, *96*, 14 330−14 335.

normal-mode analysis determines only approximate estimates of the solute entropy.

To include the influence of higher levels of theory in the energetic description of the relative energy between the **TEM1-BP** and **TEM1-BP-2** models, we also performed single-point B3LYP/6-31+G** ($E_{B3LYP6-31+G**}$) and standard AM1 (E_{AM1}) calculations on small subsystems which consisted of the side chains of Glu166 and Lys73 (H-link atoms were attached to the corresponding Cβ atoms). The computed value for the energy difference ($E_{B3LYP/6-31+G**} - E_{AM1}$) is a high level correction in the global heat of formation (H_f^0). The B3LYP/6-31+G** calculations were done using the Gaussian 98 package of programs.[44,59]

Finally, we combined the corresponding heat of formation of the solute (H_f^0), the correction term $E_{B3LYP/6-31+G**} - E_{AM1}$, the normal-mode entropy of the solute (TS^0) and its solvation energy (ΔG^0_{solv}) in order to estimate the free energy of the enzyme−substrate subsystems

$$G^0 \approx H_f^0 + (E_{B3LYP/6-31+G**} - E_{AM1}) - TS^0 + \Delta G^0_{solv}$$

The different energy terms in G^0 were averaged along 50 snapshots for each of the two configurations. We note that this computational protocol is similar to the so-called molecular-mechanics Poisson−Boltzmann surface-area (MM-PBSA) approach that takes solute configurations from MD trajectories with explicit solvent and combines the molecular mechanics energy of the solute with the free energy of solvation from PBSA calculations.[60] It may be interesting to note that although the MM-PBSA approach has intrinsically much larger errors than free energy perturbation/thermodynamic integration methods, it predicts ΔG values in respectable agreement with experiment.[61]

Results

RMSD Values and RMS Flexibility. The TEM-1 enzyme is a medium-sized globular protein with two domains. The first one is an α/β domain which comprises a five stranded β-sheet into which three α-helices (h1, *h*10 and *h*11) are packed toward the solvent interface.[24] The second domain consists of eight helices (h2−h9) located on the other side of the pleated β-sheet. The α and α/β domains are connected through two *hinge* regions in which H-bonds and salt bridges prevent any large conformational changes. The active site of the protein is located in a large depression at the interface between both domains and is readily accessible to solvent. The catalytically important residues are located on one helix-turn (Ser70 and Lys73), on a short loop in the all α-domain (Ser130), on the innermost strand of a β-sheet (Lys234, Ala237) and on the so-called Ω-loop (Glu166, Asn170) in the all α-domain.

The heavy atom root-mean-squared deviations (RMSD) of the simulated TEM-1 β-lactamase protein relative to the 1BLT crystal structure are given in Table 1. In all the simulations the RMSD value was, on average, ~1.3 Å. These figures indicate that the structural changes in the protein were not large during the course of the simulations. By superimposing the average protein structure from the **TEM1** simulation upon the initial X-ray structure, we observed that the largest deviations arise in the protein loops and the solvent exposed α-helixes (see Figure 1).

Table 1. Summary of the RMS Deviations, Radius of Gyration, and RMS Fluctuations[a]

	TEM1	TEM1-BP	TEM1-BP-2
	RMSD		
total	1.30 ± 0.15	1.27 ± 0.04	1.30 ± 0.06
backbone	0.92 ± 0.11	0.82 ± 0.06	0.84 ± 0.06
subdomain α/β	1.14 ± 0.12	1.20 ± 0.07	1.24 ± 0.07
subdomain α	1.28 ± 0.16	1.21 ± 0.05	1.21 ± 0.05
loop Ω	0.98 ± 0.07	1.00 ± 0.09	1.00 ± 0.08
	Rad_{Gyr}[b]		
	17.82 ± 0.04	17.79 ± 0.04	17.80 ± 0.04
	RMSF		
total	0.83 ± 0.07	0.75 ± 0.05	0.86 ± 0.05
backbone	0.60 ± 0.06	0.55 ± 0.05	0.66 ± 0.05
subdomain α/β	0.74 ± 0.06	0.70 ± 0.06	0.84 ± 0.07
subdomain α	0.82 ± 0.08	0.74 ± 0.06	0.82 ± 0.06
Ω loop	0.64 ± 0.07	0.62 ± 0.10	0.66 ± 0.07

[a] All data are given in Angstroms. [b] X-ray value = 18.1.

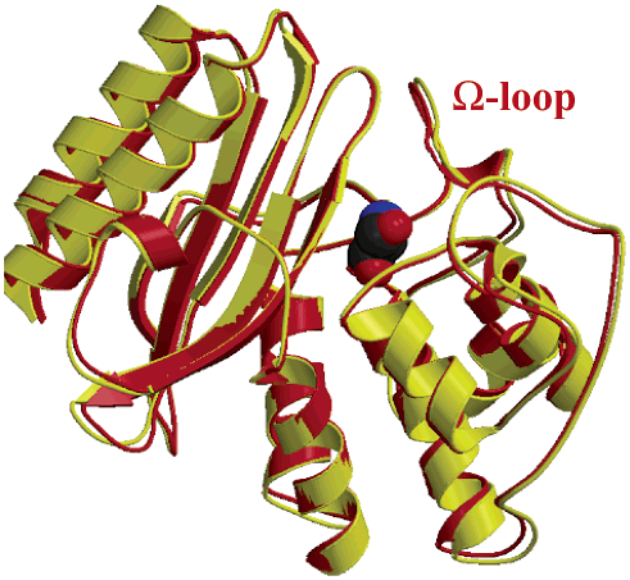

Figure 1. Superposition of ribbon models derived from the average structure of the TEM-1 enzyme during the **TEM1** simulation (in red) and the 1BLT crystallographic structure (in yellow). Ser70 is represented by vdW spheres.

At this point, it is worthwhile to compare our results for the TEM-1 enzyme with those for the PC1 enzyme from the 180-ps MD simulation reported by Vijayakumar et al.[8] The deviation of the PC1 protein from the crystal structure was much larger (~2.5 Å) than what we observed for the TEM-1 enzyme (~1.3 Å). For the PC1 enzyme, the largest RMS deviations arise from a conformational transition of the Ω loop linked to the rupture of an important salt bridge between Arg164 and Asp179 during the simulation (see below).

Figure 2 shows the time evolution of the RMS deviation of the instantaneous structures from the crystal structure for the **TEM1** and **TEM1-BP** configurations. Although the average RMSD values of both configurations are practically identical, the RMSD profile for **TEM1** fluctuates more widely than that for **TEM1-BP** throughout the MD trajectory. This is also reflected in the RMS flexibility (RMSF) of the whole protein as calculated by comparing the instantaneous protein structure to the average one (see Table 1). The calculated RMSF values for the entire protein in the **TEM1** and **TEM1-BP** models had values of 0.83 ± 0.07 and 0.75 ± 0.05 Å, respectively. The

(59) Becke, A. D. *Exchange-Correlation Approximation in Density-Functional Theory*; Yarkony, D. R., Ed.; World Scientific: Singapore, 1995.
(60) Wang, W.; Donini, O.; Reyes, C. M.; Kollman, P. A. *Annu. Rev. Biophys. Biomol. Struct.* **2001**, *30*, 211−243.
(61) Kollman, P. A.; Massova, I.; Reyes, C.; Kuhn, B.; Huo, S.; Chong, L.; Lee, M.; Lee, T.; Duan, Y.; Wang, W.; Donini, O.; Cieplak, P.; Srinivasan, J.; Case, D. A.; Cheatham, T. E. *Acc. Chem. Res.* **2000**, *33*, 889−897.

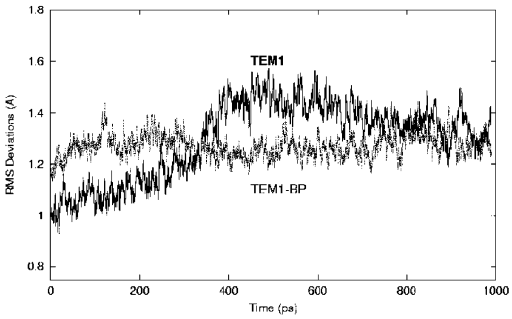

Figure 2. RMS Deviation between the instantaneous computed structures and the crystal structure for the TEM-1 enzyme as a function of time in the **TEM1** and **TEM1-BP** simulations.

Table 2. Average Distances (Å) between Heavy Atoms Corresponding to Selected Salt Bridges in TEM-1

distance	TEM1	TEM1-BP	TEM1-BP-2
Nϵ@Arg61···Oϵ2@Glu37	2.80 ± 0.11	2.80 ± 0.11	2.83 ± 0.12
Nη1@Arg61···Oϵ2@Glu64	3.07 ± 0.29	2.90 ± 0.22	5.41 ± 0.91
Nη1@Arg43···Oϵ1@Glu64	2.84 ± 0.29	2.89 ± 0.28	4.86 ± 0.19
Nϵ@Arg161···Oδ1@Asp163	2.88 ± 0.12	2.86 ± 0.12	2.84 ± 0.11
Nη2@Arg164···Oδ2@Asp179	2.76 ± 0.10	2.76 ± 0.10	2.77 ± 0.10
Nϵ@Arg164···Oδ2@Asp179	2.75 ± 0.08	2.74 ± 0.08	2.75 ± 0.08
Nϵ@Arg178···Oδ2@Asp176	3.13 ± 0.26	2.98 ± 0.19	3.04 ± 0.21
Nϵ@Arg222···Oδ1@Asp233	3.03 ± 0.18	2.96 ± 0.17	2.97 ± 0.18

segregation of the RMSF values into distinct structural elements shows that the whole protein has a larger flexibility in the unbound model **TEM1**. Therefore, these observations suggest that, in the presence of the substrate which is bound between the two protein domains, the TEM-1 enzyme is rigidified.

Conformation of the Ω loop and Stability of Salt Bridges. The Arg164-Asp179 salt bridge, which is invariant among class A β-lactamases, is placed at the base of the Ω loop linking the two ends of the loop. In the TEM-1 enzyme, the Ω loop has a polar character due to the presence of other salt bridge contacts (e.g., Arg161-Asp163), which constrains this region of the protein. In our simulations, the Ω loop slightly deviates from the crystal structure (RMSD = 0.98 ± 0.07 Å, 1.00 ± 0.09 Å for the **TEM1** and **TEM1-BP** models, respectively) and has a RMS flexibility similar to that of the rest of the protein. The direct salt bridge interaction between Arg164 and Asp179 at the base of the Ω loop was stable, with an average Nϵ@Arg164···Oδ2@Asp179 separation of ∼2.8 Å. Similarly, other salt bridge interactions present in the Ω loop and the *hinge* regions of the protein (Arg61···Glu37, Arg43-Glu64, and Arg222-Asp233) were also stable in the **TEM1** and **TEM1-BP** models (see Table 2). The stability of these contacts, which are important for the relative conformation of the protein domains and the Ω loop, is in agreement with the moderate RMSD and RMSF values of the **TEM1** and **TEM1-BP** models.

Structure of the Active Site in the TEM1 Model. A typical snapshot of the active site region and a schematic representation of the most important interresidue contacts observed during the **TEM1** MD simulation are shown in Figure 3. The mean values for some of the significant interatomic distances between heavy atoms for selected H-bond contacts are summarized in Table 3. The extent of water penetration and solvent ordering is determined by calculating the pair distribution functions $g(r)$ around selected atoms of the polar residues. The first peak position of $g(r)$ and its integrated value are collected in Table S1 in the Supporting Information.

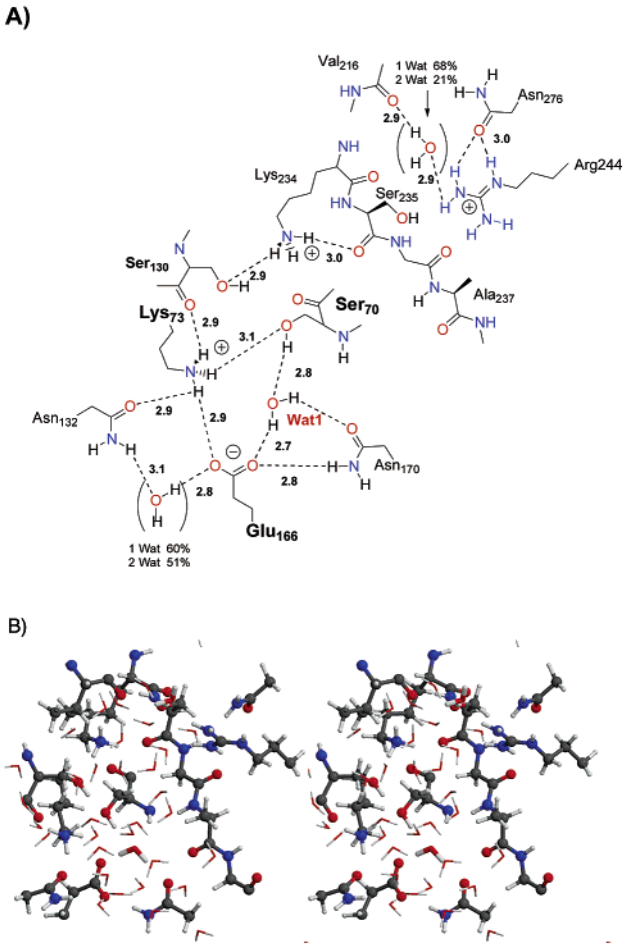

Figure 3. (a) Schematic representation of the most important interactions characterizing the active site of the **TEM1** model. (b) Stereoview of a snapshot of the **TEM1** active site.

Table 3. Summary of Some Significant Interatomic Distances (Å) in the Active Site of TEM-1 Observed during the MD Simulations[a]

interactions	TEM1	TEM1-BP	TEM1-BP-2
Oγ@Ser70···Oγ@Ser130	3.43 ± 0.46 (3.5, *3.1*)	4.14 ± 0.34	3.46 ± 0.22
Oγ@Ser70···Oϵ2@Glu166	3.78 ± 0.50 (4.2, *4.2*)	3.88 ± 0.36	4.78 ± 0.29
Oγ@Ser70···Nζ@Lys73	3.11 ± 0.61 (2.9, *2.8*)	2.88 ± 0.14	2.74 ± 0.11
Oγ@Ser70···Nζ@Lys234	4.50 ± 0.51 (4.7, *2.8*)	4.71 ± 0.26	2.87 ± 0.12
Oγ@Ser130···Nζ@Lys73	3.94 ± 0.87 (4.2, *3.6*)	5.66 ± 0.32	4.96 ± 0.27
Oγ@Ser130···Nζ@Lys234	2.94 ± 0.17 (2.9, *2.8*)	2.76 ± 0.08	2.80 ± 0.10
Oϵ1@Glu166···Nδ@Asn170	2.81 ± 0.11 (3.0, *2.9*)	3.25 ± 0.98	3.15 ± 0.48
Oϵ2@Glu166···Nζ@Lys73	2.90 ± 0.20 (3.4, *3.4*)	2.81 ± 0.14	3.76 ± 0.36
Nζ@Lys73···O@Ser130	2.91 ± 0.22 (3.3, *3.0*)	2.78 ± 0.12	3.22 ± 0.26
Nζ@Lys73···Oδ@Asn132	2.88 ± 0.16 (3.0, *2.8*)	2.86 ± 0.15	3.04 ± 0.26
Nζ@Lys234···O@Ser235	3.02 ± 0.42 (3.0, *2.8*)	2.96 ± 0.36	2.85 ± 0.12
Nη2@Arg244···Oδ@Asn276	2.94 ± 0.21 (3.0, *3.9*)	2.88 ± 0.15	2.91 ± 0.18

[a] X-ray values (in parentheses) were obtained from the 1BLT and 1XPB PDB structures.

In general, the complex hydrogen-bonding network found in the active site of the crystal structures[24,62] is well reproduced by the **TEM1** model. This H-bonding network interconnects the catalytically important residues (Ser70, Glu166, Lys73, Ser130, Lys234, Arg244, etc.) and some solvent molecules, especially Wat1 (see Table 3 and Figure 3A). The largest discrepancies between the X-ray data and the MD analyses appear in the relative position of the Lys73 ammonium group.

(62) Fonzé, E.; Charlier, P.; To'th, Y.; Vermiere, M.; Raquet, X.; Dubus, A.; Frère, J.-M. *Acta Crystallogr., Sect. D* **1995**, *51*, 682−694.

Although Lys73 gives a short and stable salt bridge interaction with Glu166 throughout the **TEM1** trajectory (Oϵ2@Glu166$\cdots$Nζ@Lys73 = 2.90 ± 0.20 Å), X-ray data show a Lys73-Glu166 ionic contact, which is significantly longer (~3.4 Å). However, it must be noted that, in the X-ray structures, a sulfate anion interacting closely with Ser130 also affects the position of the Lys73 side chain and, therefore, it is quite likely that the Lys73-Glu166 salt bridge would be strengthened in aqueous solution as indicated by the MD simulations.

Inspection of the average values for the heavy atom separations (X$\cdots$Y) and their statistical fluctuations in Table 3 helps us determine the strength and flexibility of the key interresidue contacts in aqueous solution. In particular, the Lys73-Glu166 salt bridge is buttressed by short and stable H-bond contacts involving the acetamide side chains of Asn132 and Asn170, the hydroxyl group of the essential Ser70, and several water molecules (see Figure 3). In solution, the pattern of H-bonds around Lys73 and Glu166 is similar to that in the crystal structure. Specifically, we found that the following contacts, which were present in the initial X-ray structure, were stable throughout the simulations. (1) Interactions between the ammonium group of Lys73 with the carbonyl of the Asn132 side chain and the Ser70 hydroxyl group; (2) the direct hydrogen bond between the side chain of Asn170 and the Glu166 carboxylate; and (3) the water bridge connecting the hydroxyl group of Ser70 with the Glu166 carboxylate via Wat1. However, some differences were also observed: no direct H-bonds between Asn132 and Glu166 in solution where observed, which is in disagreement with the X-ray structure. In our simulation, Asn132 and Glu166 interact through a water molecule that readily interchanges with bulk solvent (see Figure 3). The presence of some water molecules in the Lys73-Glu166 polar cluster is also observed in the pair distribution functions $g(r)$ around selected atoms (Oϵ@Glu166, Nδ@Asn132, etc.). Integration of the $g(r)$ plot out to the first minimum, indicates that there are about ~1−2 water molecules at ~2.7 Å in the first solvation layer for Glu166 corresponding to the bridging water molecules. The Lys73 ammonium group lacks a first solvation layer since its *g(r)* has its first peak centered at 4.35 Å.

Another sequence of H-bonds, which were stable in aqueous solution, interconnects the Ser130 hydroxyl group, the Lys234 ammonium group, and the O@Ser235 atom (see Figure 3). This linear sequence of H-bonds is linked to the polar cluster around the Lys73-Glu166 pair because the backbone carbonyl group of Ser130 interacts with the Lys73 ammonium group (O@Ser130$\cdots$Nζ@Lys73 = 2.91 ± 0.22 Å). In addition, the Ser130−Lys234−Ser235 cluster is solvent accessible. Thus, the *g(r)* function for the Oγ, Nζ, and Oγ atoms of Ser130, Lys234, and Ser235, show peaks around 2.8−2.9 Å with integrated values of 1.9, 1.8, and 4.1, respectively. The coordination number for the Ser235 hydroxyl group corresponds to that typically found for solvent exposed residues. Other polar groups in the active site, the Arg244 guanidinium and the backbone amide of Ala237 (the "oxyanion hole"), are mainly stabilized by H-bonds with surrounding water molecules. In addition, the presence of a water bridge connecting the Arg244 guanidinium group with the carbonyl group of Val216 is of particular interest given that a structurally conserved water molecule anchored by Val216 and Arg244 has been proposed to play an important role as a source of a proton in the inactivation of class A β-lactamases by clavulanic acid and carbapenems.[63] In the **TEM1** simulation, the first hydration shell of the Nη2@Arg244 and the O@Val216 atoms overlap to form long-lived Nη2$\cdots$$(H_2O)_n$$\cdots$O water bridges with n = 1 and 2 in 68 and 21% of the simulation snapshots (see Figure 3). The calculated lifetimes for these water bridges ranged from 0.5 to 10 ps because bulk water molecules diffuse in and replace existing water molecules in the bridge.

Table 4. Summary of the Average Distances between Heavy Atoms (Å) and Percent Occurrence Data for Important Hydrogen Bonding Interactions between Benzylpenicillin and TEM-1

	TEM1-BP		TEM1-BP-2	
H-bond	X$\cdots$Y	%	X$\cdots$Y	%
BP−O12$\cdots$H−Oγ-Ser130	2.65 ± 0.11	100.0	2.64 ± 0.10	100.0
BP−O12$\cdots$H−Oγ-Ser235	2.82 ± 0.18	100.0	2.74 ± 0.14	100.0
BP−O12$\cdots$H−Nζ-Lys234	3.59 ± 0.29	53.0	3.80 ± 0.17	16.0
BP−O13$\cdots$H−Oγ-Ser235	2.91 ± 0.19	100.0	3.04 ± 0.20	99.6
BP−O13$\cdots$H−Nη1-Arg244	2.79 ± 0.12	100.0	2.74 ± 0.09	100.0
BP−O8$\cdots$H−N−Ser70	3.38 ± 0.27	96.4	3.78 ± 0.17	59.0
BP−O8$\cdots$H−N−Ala237	2.86 ± 0.11	100.0	2.88 ± 0.12	100.0
BP−O8$\cdots$H−O−Wat1	3.26 ± 0.31	0.9	2.97 ± 0.22	58.0
Ala237−C=O$\cdots$HN14−BP	3.10 ± 0.22	48.2	3.42 ± 0.24	0.1
BP−O16$\cdots$H−Nδ-Asn132	2.98 ± 0.20	95.3	3.04 ± 0.23	98.2
BP−O16$\cdots$H−O−Wat1	3.51 ± 0.40	22.1	2.90 ± 0.26	98.5

When we compare the structure of the active site that emerges from the **TEM1** model with previously reported results,[8] the most striking difference is in the dynamics of the polar cluster around Lys73-Glu166. In the PC1 simulation, the hydroxyl group of Ser70 and the Oϵ1@Glu166 atom formed a short H-bond (Oϵ1@Glu166$\cdots$Oγ@Ser70 ~ 2.8 Å) and the hydrolytic Wat1 molecule was forced to move away from Ser70, that is, the Glu166-Wat1-Ser70 clustering was unstable. This rearrangement of the H-bonding network observed in the PC1 X-ray structure was linked to the large mobility of the Ω loop. In our simulation, the Glu166−Wat1−Ser70 association was stable throughout the **TEM1** simulation (see above). Most interestingly, the Wat1 molecule did not exchange with other (bulk) water molecules. This means that the predicted half-life for the Glu166−Wat1−Ser70 water bridge would be relatively long (>1 ns).

Enzyme−Substrate Binding Determinants in the TEM1-BP Model. A snapshot of the active site of the TEM-1 enzyme complexed with benzylpenicillin is given in Figure 4. Figure 4 also schematically shows the most significant H-bond and hydrophobic contacts between the substrate and the enzyme residues. In Table 4, the H-bond contacts are characterized in terms of distances between heavy atoms and their percentage of occurrence.

The overall protein architecture of the **TEM1-BP** model is almost identical to **TEM1** because the RMSD of **TEM1-BP** with respect to the average **TEM1** structure is only 0.91 Å (0.71 Å backbone). However, as indicated above, the presence of the substrate in **TEM1-BP** results in a moderate decrease of the protein flexibility with respect to the unbound model **TEM1**.

In the active site region, we found that changes in the interresidue contacts and the flexibility of the amino acid side chains were not large upon substrate binding. For example, the polar cluster around the Lys73−Glu166 pair including the Glu166−Wat1−Ser70 bridge as well as the Ser130−Lys234−Ser235 H-bonding sequence, were stable in the presence of the

(63) Imtiaz, U.; Billings, E. M.; Knox, J. R.; Manavathu, E. K.; Lerner, S. A.; Mobashery, S. *J. Am. Chem. Soc.* **1993**, *115*, 4435−4442.

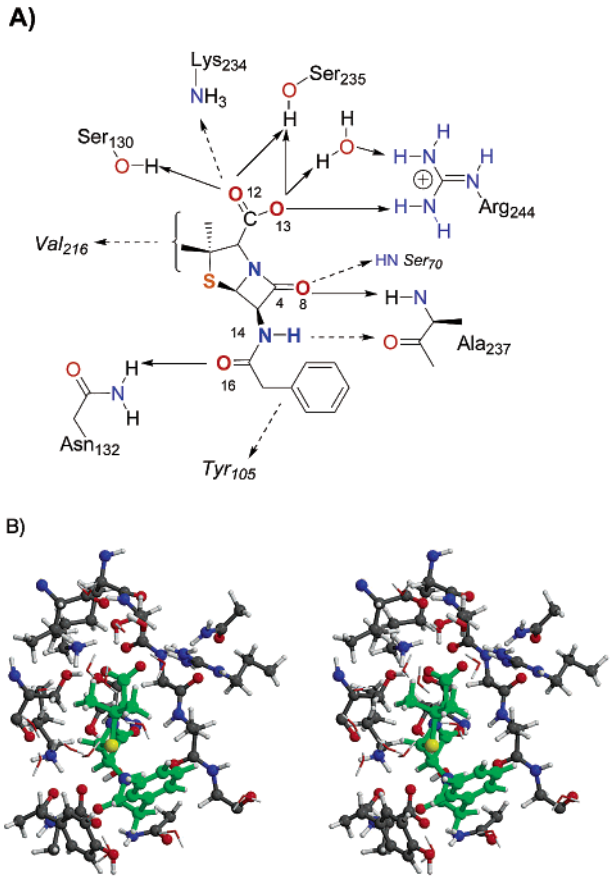

Figure 4. (a) Schematic representation of the enzyme−substrate binding determinants between benzylpenicillin and the TEM-1 enzyme. Numbering of the benzylpenicillin atoms. (b) Stereoview of a snapshot of the **TEM1-BP** active site with benzylpenicillin shown in green.

substrate. Indeed, this suggests that the **TEM1** model evolves in a conformation suitable for accommodating the benzylpenicillin substrate. However, it is also interesting to note that some of the interresidue H-bonds are strengthened in the presence of the substrate, most likely due to the partial desolvation of the active site region. This is the case for the Oγ@Ser70···H−Nζ@Lys73 H contact which has a stable O···N distance (2.88 ± 0.14 Å) throughout the **TEM1-BP** trajectory.

As expected, the presence of the substrate desolvates the polar residues in the active site. For the less solvent accessible residues, Lys73, Glu166, and Ser70, the only solvent molecule close to their side chains is Wat1 bridging the Glu166 carboxylate and the Ser70 hydroxyl groups. Wat1 was buried underneath the benzylpenicillin substrate throughout the simulation. On the other hand, the first solvation shell centered on Oγ@Ser130 was nearly devoid of solvent molecules (the corresponding $g(r)$ function peaks at 3.69 Å). The rest of the polar groups (Lys234, Ser235, and Arg244) were also desolvated although they remain solvent accessible (see Figure 4). Of course, the formation of long-lived enzyme−substrate contacts compensates for the loss of active site solvation.

The thiazolidine ring of the substrate was in the equatorial conformation throughout the **TEM1-BP** trajectory. In terms of the Cremer−Pople parameters, the mean values of the puckering amplitude and the phase angle were 0.47 ± 0.06 Å and 95 ± 6°, respectively. In the starting enzyme−substrate complex, the puckering of the thiazolidine moiety corresponded to the axial conformer. However, the puckering of this ring changed rapidly into the equatorial conformation during the equilibration phase of the simulation. Because the molecular mechanics representation used for benzylpenicillin reproduces the conformational properties of the substrate both in the gas-phase and in aqueous solution, we conclude that the active site of the TEM-1 β-lactamase binds preferentially to the equatorial conformer of penicillins. In effect, the equatorial conformation of the BP substrate avoids a possible steric clash with the methyl group of Ala237 and simultaneously favors the direct interaction between the substrate carboxylate and Arg244 (see below).

As shown in Figure 4, the three structural parts of the benzylpenicillin antibiotic (i.e., the five-membered thiazolidine ring, the four-membered β-lactam ring and the 6-acylamino side chain) contribute to anchor the substrate to the active site cleft:

(1) In the thiazolidine ring of BP, the methyl groups are oriented toward the hydrophobic side chain of Val216. Simultaneously, the negatively charged carboxylate group interacts with an array of polar and charged residues: Ser130, Lys234, Ser235, and Arg244. In terms of the X···Y distances of the corresponding H-bonds, the shortest H-bond was the Oγ@Ser130···O12@BP interaction (2.65 ± 0.11 Å), whereas the weakest interaction corresponds to the BP−COO$^-$···$^+{}_3$HN-Lys234 contact (~3.6 Å), which is present in only 53% of the computed trajectory. The Ser235 hydroxyl group has a bifurcated H-bond with both O atoms of the BP carboxylate group (Oγ@Ser235···O@BP ~2.8−2.9 ± 0.2 Å). In addition, one of the amino ends of the Arg244 side chain has a direct Nη1−H···O13@BP contact (2.79 ± 0.12 Å). The other amino end of Arg244 is water bridged simultaneously to the O13@BP atom and the Val216 carbonyl group through one water molecule. The persistence of this water bridge is very high when the substrate is present (96% of the analyzed snapshots show the Nη2···(H_2O)···O=C interaction with an average life of ~100 ps). The stability of this association, which is clearly important for substrate binding, is in agreement with its proposed role in the opening of the five-membered ring of clavunalate inhibitors and carbapenems.[63]

(2) In the β-lactam ring, the BP carbonyl group is oriented toward the H−N bond of the backbone amide of Ala237. This results in a short (2.86 ± 0.11 Å) and very stable (100%) C=O···H−N bond. A weaker H-bond interaction of the BP carbonyl group is formed with the Ser70 main chain amide (3.38 ± 0.27 Å, 96%).

(3) To bind the side chain of BP, the most important specific interaction was the C=O···H−N H-bond formed between the acylamino carbonyl group and the amino group of the Asn132 side chain. This long-lived interaction had an average O···N distance of 2.98 ± 0.20 Å. A weak hydrogen bond is formed between the N14@BP atom and the Ala237 carbonyl group, which results in an average N14···O distance of 3.10 ± 0.22 Å. We also characterized the hydrophobic interactions between the $-CH_2-$Ph moiety of BP and Tyr105 on the basis of the distance involving the center of mass of the Tyr105 side chain and the benzyl group of BP. The resultant value (5.1 ± 0.4 Å) indicates that the motions of both aromatic rings are correlated during the dynamics although they do not form a close $\pi-\pi$ contact (see Figure 4).

The analyses of the **TEM1-BP** simulation show that binding of the BP substrate occurs without substantially altering the

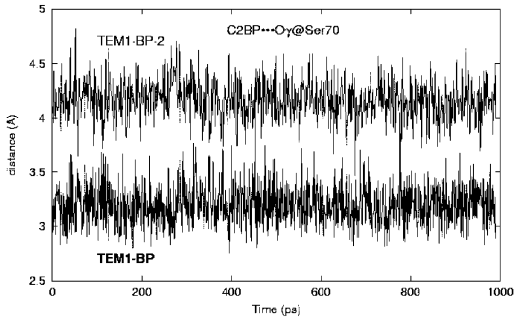

Figure 5. Separation (Å) between the C4 atom of benzylpenicillin and the Oγ atom of Ser70 during the **TEM1-BP** and **TEM1-BP-2** simulations.

Table 5. Average Heats of Formation, Solvation Energies and Entropic Contributions in kcal/mol of the Protein Subsystems Constructed from the **TEM1-BP** and **TEM1-BP-2** Configurations[a]

	H_f^0	ΔG^0_{solv}	$-T\Delta S^0$
TEM1-BP	-2420 ± 36	-581 ± 15	-695 ± 3
TEM1-BP-2	-2409 ± 38	-603 ± 21	-696 ± 3
	(*11*)	(*−22*)	(*−1*)

	$E_{B3LYP/6-31+G^{**}}$	E_{AM1}
L73-NH_3^+···$^-$OOC-E166	-482.1953 ± 0.0030	-91 ± 1
L73-NH_2···HOOC-E166	-482.2355 ± 0.0012	-134 ± 8
	(*−25*)	(*−43*)

[a] Relative differences between the **TEM1-BP-2** mean values with respect to the **TEM1-BP** values are in parentheses. Average energies ($E_{B3LYP/6-31+G^{**}}$ in au; E_{AM1} in kcal/mol) for the Glu166 and Lys73 side chains are also indicated.

conformation of the catalytically important residues. However, is the Michaelis complex represented by the **TEM1-BP** model compatible with a fast catalysis? To address this, we analyzed the **TEM1-BP** trajectory by monitoring the distance between C4@BP of the β-lactam carbonyl group (electrophile) and Oγ@Ser70 (nucleophile). Interestingly, the mean value for this distance was low, 3.19 ± 0.18 Å, with the closest distance being only 2.68 Å. Figure 5 shows a plot of the Oγ···C4 separation indicating that this distance fluctuates quite smoothly around its average value. The average Ser70@Cβ-Oγ···C4@BP angle is $98.6 \pm 7.2°$, which is close to those observed for typical C−O−C bond angles. Thus, the nucleophile in the **TEM1-BP** simulation is well positioned to attack the carbonyl carbon of the substrate.

Structure and Dynamics of the Michaelis Complex After a Lys73→Glu166 Proton Transfer. It has been proposed that the generation of an unprotonated Lys73 residue could be accomplished by a proton transfer between Lys73→Glu166 in the presence of the substrate. In this way, Lys73 could act as the general base by abstracting a proton from the Ser70 hydroxyl group. To examine the structural and dynamic consequences of a Lys73→Glu166 proton transfer, we carried out the **TEM1-BP-2** simulation in which the side chains of Lys73 and Glu166 were neutralized, whereas the rest of the active site residues were in the **TEM1-BP** configuration. Figure 6 shows the structure of the active site region in the **TEM1-BP-2** state. Other data (RMSD and RMSF values, mean X···Y distances, etc.) are collected in Tables 1−5.

The **TEM1-BP-2** simulation gives RMSDs that hardly differ from those observed for the **TEM1-BP** model. In contrast, the RMS flexibility discriminates between both models: the **TEM1-BP-2** trajectory gives RMSF values for all heavy (0.86 ± 0.05 Å) or backbone atoms (0.66 ± 0.05 Å) that are closer to those

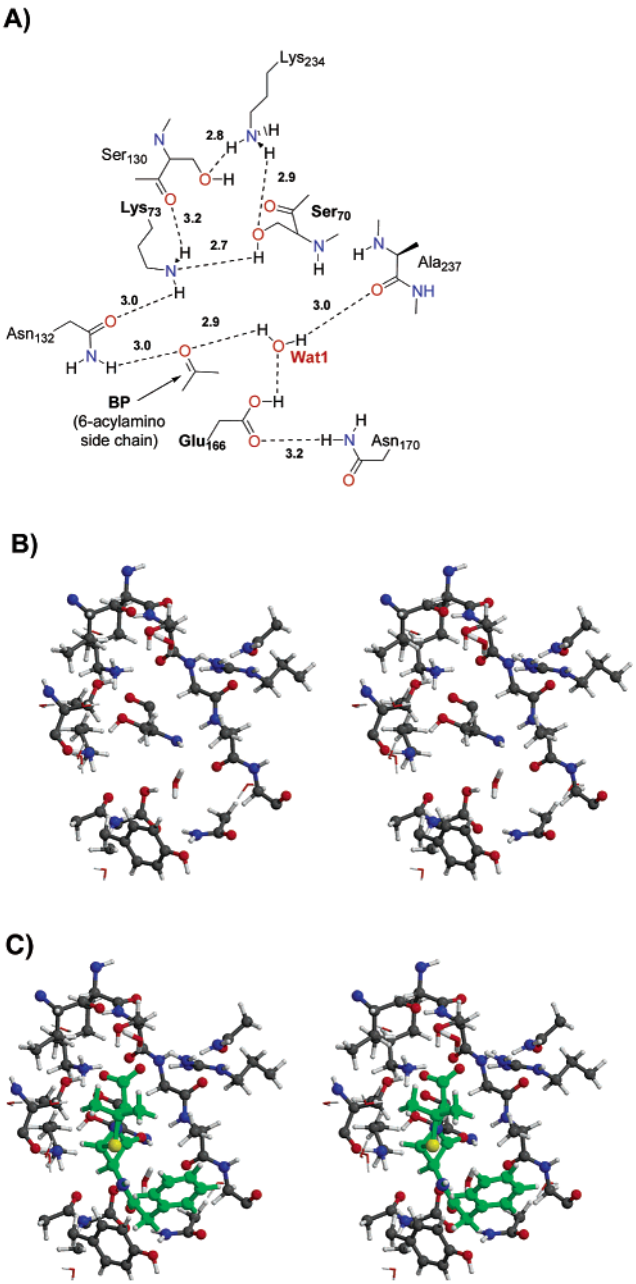

Figure 6. (a) Schematic representation of several interresidue contacts characterizing the active site of the **TEM1-BP-2** model. (b) Stereoview of a snapshot of the **TEM1-BP-2** active site (benzylpenicillin not shown). (c) Stereoview of a snapshot of the **TEM1-BP-2** active site with benzylpenicillin shown in green.

of the unbound model **TEM1**. Therefore, the global flexibility of the complexed form of TEM-1 increases when the Lys73−Glu166 salt bridge is lost. However, we observed that the RMS flexibility of the important residues in the active site do not significantly differ between the **TEM1-BP** and **TEM1-BP-2** states.

The interresidue contacts in the active site change in response to the neutralization of the Lys73 and Glu166 side chains. The most important changes occur in the contacts and relative positions of Lys73, Ser70, Glu166, Asn132, and Asn170 (i.e., the residues which were clustered in the **TEM1** and **TEM1-BP** models), whereas the interactions between Ser130···Lys234···Ser235 were less affected (see Figures 3A and 6A). Specifically,

we found that: (1) the Glu166 carboxylic group is stabilized by Glu-COOH···OH_2 (Wat1) and Glu-C═O···NH_2−CO−Asn170 H-bond contacts. (2) The Glu166-Wat-Ser70 water bridge is lost. In **TEM1-BP-2** Wat1 links the backbone carbonyl group of Ala237 with that of the 6-acylamino side chain of BP. (3) The hydroxyl group of the essential Ser70 residue bridges the Lys73 amino and Lys234 ammonium groups through long-lived Lys234-NH_4^+···OH(Ser70)···NH_2-Lys73 interactions. The mean Oγ@Ser70···Nζ@Lys73 distance amounts to 2.74 ± 0.11 Å, the hydroxyl group of Ser70 being the proton donor in this H-bond interaction.

Given that Asn132 is the only residue in the polar cluster around the Lys73−Glu166 pair, which is involved in substrate binding, it turns out that the **TEM1-BP** and **TEM1-BP-2** models have very similar enzyme−substrate interactions. Thus, in Figure 6 and Table 4 we see that contacts between the BP carboxylate and the nearby residues (Ser130, Ser235, Arg244) were stable in the **TEM1-BP-2** trajectory. Similarly, the H-bond between the β-lactam carbonyl and Ala237 is also stable. However, the 6-acylamino side chain of BP readjusts its positioning in response to the **TEM1-BP→TEM1-BP-2** conversion. Although the Asn132-$CONH_2$···O═C(BP) interaction is maintained, the weak BP−N14−H···O═C−Ala237 hydrogen bond is nearly lost, whereas the side chain carbonyl of BP also interacts with Wat1. Simultaneously, the hydrophobic clustering of the BP benzyl ring with the Tyr105 side chain is more compact: the center of mass of the aromatic rings are 4.9 ± 0.3 Å apart and movements of the Tyr105 side chain are damped out (the RMS flexibility of Tyr105 is reduced from 0.62 ± 0.27 Å in the **TEM1-BP** model to 0.25 ± 0.07 Å in **TEM1-BP-2**).

From our analyses, it is clear that the **TEM1-BP→TEM1-BP-2** conversion preserves the important substrate binding interactions and results in a stable Ser70-OH···NH_2-Lys73 H-bond which is adequate for the unprotonated Lys73 to be the general base catalyst. However, it is also interesting to analyze the relative abundance of near attack conformations in the **TEM1-BP-2** state in terms of the Oγ@Ser70···C4@BP distance. Figure 5 also plots the evolution of the reactive distance in the **TEM1-BP-2** model. This interaction has an average value of 4.17 ± 0.18 Å with a lower bound of 3.46 Å This average distance is ∼1 Å longer than that in the **TEM1-BP** model. In addition, the Ser70@Cβ-Oγ···C4@BP angle is low (59.2 ± 6.0°). This means that proton transfer from Lys73 to Glu166 shifts the carbonyl group of the β-lactam ring away from the attacking hydroxyl group of Ser70. Hence, the **TEM1-BP** configuration is more favorable than **TEM1-BP-2** for nucleophilic attack. However, we expect that nucleophilic attack would not be entirely impeded in the **TEM1-BP-2** state because many of the analyzed structures (∼17%) have Oγ@Ser70···C4@BP distances below 4.0 Å.

To further discriminate between the **TEM1-BP** and **TEM1-BP-2** models, we estimated the free energy difference between the two protein configurations in the presence of the substrate following the computational procedure described in the Methods section. Table 5 summarizes the results from different energy calculations (semiempirical, ab initio) on model systems and those from solvation free energy and entropy (normal mode) calculations. By adding the average values of the free-energy terms (i.e., $\Delta H_f^0 - T\Delta S^0 + \Delta\Delta G^0_{solv}$), it turns out that the **TEM1-BP-2** state is more favorable by about 12 kcal/mol. However, the semiempirical AM1 Hamiltonian overestimates the intrinsic stability of the neutral Lys73-NH_2 HOOC-Glu166 configuration with respect to the ionic Lys73-NH_3^+···$^-$OOC-Glu166 state by about 18 kcal/mol. Thus, when the averaged high level correction term, $\Delta(E_{B3LYP/6\text{-}31+G^{**}} - E_{AM1})$, is included, we obtain a corrected ΔG^0 value of +6 kcal/mol favoring the **TEM1-BP** configuration. This magnitude of the estimated ΔG^0 difference suggests that the **TEM1-BP** state corresponds to the ground state of the Michaelis complex between the TEM-1 enzyme and benzylpenicillin. Simultaneously, the **TEM1-BP-2** state could be also populated if the energetic fluctuations in the H_f^0 and ΔG^0_{solv} terms (±15−38 kcal/mol; see Table 5), were channeled into the Lys73 and Glu166 side chains.

Discussion

New Insight into the Structure and Dynamics of the TEM-1 β-Lactamase. From the analyses of our MD simulations for the unbound form of the TEM-1 enzyme, we concluded that the **TEM1** configuration is a good model for representing the structure and dynamics of the protein in aqueous solution. The quality of the model is reflected in the moderate RMS deviations between the simulated and experimental structure of TEM-1, the preservation of important contacts in the *hinge* regions connecting the all α and the α/β domains, etc. However, the **TEM1** simulation, not only complements the structural information provided by X-ray data,[24] but also gives new insight into the behavior of the fully hydrated protein. In this respect, the most important aspects of the **TEM1** simulation are as follows: (1) the relatively low mobility of the Ω loop, (2) the persistence of the H-bonds interconnecting the catalytically important residues and, (3) the localization of the Wat1 molecule bridging the Ser70 and Glu166 side chains.

The stability of the Ω loop in the solvated TEM-1 enzyme correlates with the presence of several ionic contacts stabilizing the loop conformation beyond the conserved Arg164−Asp179 salt bridge. This relatively "rigid" picture both in the crystal and solution states, contrasts sharply with the highly mobile Ω loop observed in the MD simulation of the PC1 β-lactamase from *S. aureus* in which the Arg164−Asp179 salt bridge was unstable.[8] Although the PC1 enzyme certainly has a more hydrophobic Ω loop, we feel that the actual dynamics of the Ω loop should not differ dramatically since this loop contains the catalytically important Glu166 residue. We also note that, in our calculations, the PME method was applied to include long-range electrostatic effects which are usually required to stabilize the conformation of highly charged biomolecules in aqueous solution. Thus, the absence of long-range corrections in the simulations of the PC1 enzyme could explain the loss of the Arg164−Asp179 contact and the large mobility of the Ω loop.

The **TEM1** simulation results in a long-lived Lys73−Glu166 salt bridge while the average distances of other important interresidue contacts were very similar in solution and in the X-ray structure. Our simulations confirm the participation of Wat1 in the structure of the active site as originally observed by the crystallographic studies of the free enzyme and molecular modeling.[23,24] In effect, we found that Wat1 is integral to the active site since the Glu166-COO^-···H_2O(Wat1)···HO−Ser70 interaction is present throughout the simulation. The observed stability of the water bridge mediated by Wat1 agrees with recent

experimental data that indicates the critical role Wat1 plays in the deacylation process in the *wild-type TEM-1* β-lactamase. Electron nuclear double resonance (ENDOR) spectroscopy under cryo conditions revealed the presence of a water molecule within hydrogen-bonding distance to the Glu166 carboxylate in the wild-type TEM-1 acylenzyme.[64] The ENDOR-active water was located ~1 Å from the site occupied by Wat1 either in the X-ray structure of the free enzyme or during the **TEM1** simulation. Altogether, the X-ray structures of the unbound TEM-1 enzyme, the **TEM1** MD simulation, and the ENDOR spectroscopic data, nicely illustrate how the Wat1 is integrated into the architecture of the active site.

Clearly, the structural relevance of Wat1 goes hand-in-hand with its crucial catalytic role as the hydrolytic water in the deacylation process. For example, the catalytic importance of Wat1 was clearly shown by the structure of the TEM-1 β-lactamase inhibited by 6α(hydroxymethyl)penicillanic acid in which the hydroxymethyl moiety of the inhibitor occupies the region near the Wat1 molecule.[41] Similarly, in the Asn170Gln mutant of the PC1 enzyme,[14] the extended side chain of the Gln residue blocks access to Wat1 and impairs deacylation. However, the PC1 mutant[14] and the Glu166Asn mutant of the TEM-1 enzyme[12] have relatively fast acylation rates (comparable with that of the native form in the case of the PC1 mutant). Therefore, an active kinetic role for the Glu166-Wat1-Ser70 association during the acylation process remains uncertain.

Substrate Binding Determinants. In previous work, the binding of benzylpenicillin to the active site of different class A β-lactamases (the enzymes from *Streptomyces albus* G, PC1 from *S. aureus* and TEM-1 from *E. coli*) has been investigated by means of energy minimization or docking analyses.[9,16,18,22,23] The important role of the Asn132 and Ala237 residues in the Michaelis complex has been observed in all the molecular modeling studies. In the same studies, however, the identity and/or relative importance of the residues interacting with the β-lactam carboxylate (Ser130, Lys234, Ser235, Arg244) were quite variable.

The **TEM1-BP** and **TEM1-BP-2** MD simulations provide new insight into the relative strength and specificity of the protein−substrate contacts. For example, the distortion of the β-lactam carbonyl group in the ground-state Michaelis Complex revealed by FTIR spectroscopy has been attributed to its hydrogen bonding to two backbone amides of Ala237 and Ser70 (the "oxyanion hole").[65] According to our simulations, the observed shift in the C═O stretch frequency is mainly due to one H-bond with Ala237 (BP−C═O···H−N−Ala237) which has a mean distance between heavy atoms of ~2.8 ± 0.1 Å, ~0.5 Å shorter than that corresponding to the weaker BP−C═O···H−N−Ser70 interaction.

The analysis of the interactions between the benzylpenicillin carboxylate and the nearby residues can be particularly relevant. As mentioned above, the thiazolidine moiety of benzylpenicillin adopted an equatorial conformation in which the negatively charged carboxylate was capable of establishing direct H-bond contacts with the hydroxyl groups of Ser130 and Ser235 and one amino end of the Arg244 guanidinium. However, the ammonium group of Lys234 played mainly an electrostatic role (i.e., there is no direct H-bond connecting Lys234 and the substrate). The simulations confirmed that the stable water bridge interconnecting the substrate carboxylate, the Arg244 side chain and the Val216 carbonyl is also important for substrate binding. Nevertheless, the most interesting residues functioning as "carboxylate anchors" are Ser130 and Arg244 because their side chains form short and persistent H-bonds with the BP carboxylate.

The role Arg244 plays in stabilizing the Michaelis complex is in agreement with the direct salt bridge between Arg244 and the substrate carboxylate found in the X-ray structures for acylenzyme intermediates of mutated class A β-lactamases.[11,42] Although earlier molecular modeling studies did not detect a direct interaction between Arg244 and the β-lactams at the pre-acylation complex, our simulations suggest that Arg244 can stabilize the benzylpenicillin substrate all along the reaction coordinate for the acylation process.

The contribution of the Ser130 hydroxyl group to positioning the substrate carboxylate seems also important. Interestingly, this ability of Ser130 seems particularly notable in the PSE−4 class A β-lactamase from *Pseudomonas aeruginosa*.[66] The PSE−4 enzyme, which preferentially hydrolyzes carbenicillins, has a point Lys234Arg mutation and an alternate conformation for Ser130 with respect to the TEM-1 enzyme. These changes help shift the substrate in the active site cleft in order to avoid a steric clash between the carbenicillin α-carboxylate group and the Asn170 side chain.[66]

Although our analyses focused on the specific interactions of the substrate carboxylate with Arg244 and Ser130, we note that the side chains of these residues are embedded in a complex network of interactions involving Lys234, Ser235 and water molecules. In fact all these groups comprise a "positively charged cluster", which is well adapted to recognize and bind the carboxylate group of penicillins. In this respect, mutagenesis experiments have shown that, although the Arg244 and Ser130 mutations have nonnegligible effects on the acylation of the TEM-1 enzyme, the mutated enzymes retain an important level of catalytic activity. For example, both the Ser130Gly and Ser130Ala TEM-1 mutants can hydrolyze benzylpenicillin efficiently, with the observed differences in the k_{cat}/K_m values arising mainly from K_m.[67] On the other hand, the Arg244Thr and Arg244Gln mutants result in impaired enzymes, having k_{cat}/K_M values which are 2−3 orders of magnitude lower than those of the wild-type enzyme.[68] Taking into account these data as well as the existence of a network of interrelated contacts in the "positively charged cluster", it may be reasonably expected that the particular role of Arg244 and Ser130 in substrate binding could be partially compensated by other polar groups or water molecules in the mutated enzymes. Thus, previous molecular modeling studies[9] have shown that, in the Ser130Gly mutant class A β-lactamases, a water molecule can be placed at approximately the same position as that occupied by the Ser130 hydroxyl group in the wild type. Similarly, the polar side chains of the threonine-244 and glutamine-244 residues in the Arg244 mutants could contribute to the binding of the substrate carboxylate either directly or through water bridges.

(64) Mustafi, D.; Sosa-Peinado, A.; Makinen, M. W. *Biochemistry* **2001**, *40*, 2397−2409.
(65) Hokenson, M. J.; Cope, G. A.; Lewis, E. R.; Oberg, K. A.; Fink, A. L. *Biochemistry* **2000**, *39*, 6538−6545.
(66) Lim, D.; Sanschagrin, F.; Passmore, L.; De Castro, L.; Levesque, R. C.; Strydnadka, N. C. J. *Biochemistry* **2001**, *40*, 395−402.
(67) Matagne, A.; Frère, J. M. *Biochim. Biophys. Acta* **1995**, *1246*, 109−127.
(68) Delaire, M.; Labia, R.; Samama, J. P.; Masson, J. M. *J. Biol. Chem.* **1992**, *267*, 20 600−20 606.

Finally, we note that the placement of the characteristic carboxylate of cephalosporins in the pre-catalytic complex with class C β-lactamases, which has been solved crystallographically for the AmpC enzyme complexed with cephalothin,[69] turns out to be very similar to the mode of carboxylate binding characterized by our simulations on the TEM-1 enzyme. The class C enzymes are better cephalosporinases than penicillinases while the TEM-1 enzyme is considered a highly proficient penicillinase. This suggests that the "cluster" of polar/charged residues around the substrate carboxylate is required for optimum catalysis in the serine β-lactamases.

Implications for the Acylation Mechanism. The enzyme−substrate complex in the **TEM1-BP** model corresponds to the ground-state Michaelis complex in which the substrate is bound by specific and long-lived enzyme−substrate interactions. Importantly, the mode of binding of benzylpenicillin is very favorable for catalysis given that the interresidue interactions linking the potentially reactive groups (i.e., Ser70, Ser130, Lys73, Glu166) are very stable. Furthermore, the β-lactam carbonyl group, H-bonded to the backbone amide of Ala237, lies very close to the hydroxyl group of the nucleophilic Ser70 with an average C4···Oγ@Ser70 distance of ∼3.2 Å. Hence, provided that a proton is abstracted from the Ser70 hydroxyl group, the nucleophilic attack can readily occur. Of course, the *crux* of the mechanistic problem is how to activate the hydroxyl group of Ser70. We discuss three possibilities for the initial proton-transfer step that could trigger the whole acylation process: (1) a Lys73-NH_3^+→$^-$OOC-Glu166 proton transfer; (2) a Ser70-OH→$^-$OOC-Glu166 transfer assisted by the bridging Wat1 molecule; (3) a Ser130-OH→$^-$OOC−BP proton transfer leading to a carboxylate and hydroxyl assisted mechanism for the acylation reaction.

As mentioned in the Introduction, the mechanistic proposal in which Lys73 acts as the general base requires that the ammonium group of Lys73 be deprotonated. In the presence of the substrate, the simplest pathway for neutralization of Lys73 would be a Lys73-NH_3^+→$^-$OOC-Glu166 proton transfer. The rearrangement of the H-bond network in response to the different charge distribution produced by this proton-transfer event, was explored by carrying out the **TEM1-BP-2** simulation in which both Lys73 and Glu166 were neutralized. We found that the main substrate-binding determinants were not altered by the Lys73→Glu166 proton transfer and a new Ser70-OH···:NH_2-Lys73 H-bond is formed which, in turn, could activate Ser70. However, other geometrical changes were less favorable for catalysis: the C4···Oγ@Ser70 separation was increased to ∼4.1 Å and Wat1 was loosely bound to the carboxylic group of Glu166. Moreover, our energetic analyses show that the **TEM1-BP** state corresponds to the ground state of the TEM-1-benzylpenicillin complex, being ∼6 kcal/mol below the **TEM1-BP-2** configuration. In fact, our calculations are in agreement with previous pK_a determinations for Lys73 in the TEM-1 enzyme using Poisson−Boltzmann methodologies.[16] These electrostatic calculations, which were carried out for different substrates including benzylpenicillin, indicated that the pK_a of Lys73 is not lowered upon substrate binding and remains above 10. Overall, we conclude that an acylation mechanism involving an active kinetic role for Lys73 is unlikely.

The **TEM1-BP** simulation confirms that activation of Ser70 by the Glu166-Wat1 moiety is favored thanks to the stable Ser70-OH···OH_2···$^-$OOC-Glu166 water bridge, which clearly pre-organizes the required proton transfer pathway. Therefore, the structure and dynamics of the TEM1-benzylpenicillin complex were compatible with the acylation mechanism assisted by both Glu166 and Wat1 as originally proposed on the basis of molecular modeling studies.[23] However, as discussed in the Introduction, this route for acylation cannot be unique and, therefore, other alternative (and competitive) mechanisms must be possible in the active site of the TEM-1 enzyme.

Another mechanism for delivering the proton from Ser70 to the leaving N atom may occur via the assistance of both the hydroxyl group of Ser130 and the substrate carboxylate group. This mechanism implies several proton-transfer steps, that is, Ser70→Ser130→COO^-(BP)→N(BP). According to the results of our MD calculations, the first proton "jump" would be, most likely, Ser130-OH→$^-$OOC−BP since the hydroxyl group of Ser130 is hydrogen-bonded to the carboxylate group of BP throughout the **TEM1-BP** simulation. Subsequently, localization of the negative charge on the Oγ@Ser130 atom could induce a rearrangement of the Ser70 hydroxyl group followed by a Ser70-OH→$^-$O−Ser130 proton transfer. Alternatively, the sequence of proton jumps, Ser70→Ser130→ COO^-(BP), could occur in a concerted fashion. It is also interesting to note that proton delivery to the leaving N atom could readily occur via the substrate carboxylate group while a more complex pathway involving the side chains of Glu166, Lys73, and Ser130 would be required for the Glu166-Wat1 assisted mechanism. The viability of the mechanism is further supported by its similarity with the mechanistic proposals for the class C β-lactamases. Thus, the crystallographic structure of the precovalent substrate complex between cephalothin and the Ser69Gly mutant of the AmpC β-lactamase,[69] shows that the substrate carboxylate accepts a hydrogen bond from Tyr150, which in turn could abstract a proton from the nucleophilic Ser64, either directly or via Lys67. For the deacylation of class C enzymes, a mechanism has been proposed in which the hydrolytic water molecule is activated by substrate-assisted catalysis.[70]

Could the Ser130 and carboxylate-assisted mechanism represent a *general* acylation pathway for class A β-lactamases? In the class A β-lactamase from *Bacillus cereus*, esterification of the carboxylate group in penicillins decreases the enzyme efficiency (k_{cat}/K_M) by a factor of ∼10^4, whereas a cephalosporin lactone is hydrolyzed 50 times faster than an analogous cephalosporin with a free carboxylate group.[71] Therefore, another proton-transfer pathway, not involving the substrate carboxylate group, should constitute a competitive kinetic route in the hydrolysis of cephalosporins.

Our MD simulations strongly suggest that both the Glu166−Wat1 pair and the hydroxyl group of Ser130 bound to the substrate carboxylate group, could accept the proton from Ser70. Hence, it is reasonable to hypothesize that the two acylation pathways would be competitive. Kinetic preference for one mechanism or the other, would depend on the nature of the substrate (e.g., penicillins vs cephalosporins) and/or on the presence of point mutations. In this scenario, acylation of the

(69) Beadle, B. M.; Trehan, I.; Focia, P. J.; Shoichet, B. K. *Structure* **2002**, *10*, 413−414.

(70) Bulychev, A.; Massova, I.; Miyashita, K.; Mobashery, S. *J. Am. Chem. Soc.* **1997**, *119*, 7619−7625.

(71) Laws, A. P.; Page, M. I. *J. Chem. Soc., Perkin Trans. II* **1989**, 1577−1581.

TEM-1 enzyme by the boronic acid inhibitor, which lacks the carboxylate group interacting with Ser130, should proceed through protonation of Glu166 as experimentally observed.[10] On the other hand, class A β-lactamases (in their native or mutant forms) as well as other serine proteases could be acylated with the assistance of the nonnucleophilic serine (Ser130 in TEM-1) and the substrate carboxylate group.

Summary

MD simulations of the fully hydrated TEM-1 β-lactamase using the AMBER force field and long-range electrostatic corrections provided insights regarding the structure and dynamics of the protein in aqueous solution. For the free enzyme, the important salt bridge contacts and the conformation of the Ω loop originally observed in the X-ray structure remain stable throughout the simulation. The interresidue contacts defining the complex H-bond network in the active site were also very stable, especially the polar cluster surrounding the Lys73−Glu166 salt bridge. The one-water bridge connecting Glu166 and Ser70 is a long-lived interaction, which emphasizes the structural and catalytic relevance of Wat1. In the simulations of the TEM1-benzylpenicillin Michaelis complex, the presence of the substrate weakly affects the interresidue contacts characterizing the unbound state. Ser130, Ser235, and Arg244 directly interact with the substrate carboxylate via H-bonds whereas the Lys234 ammonium group has an electrostatic influence. These interactions together with other specific contacts (e.g., (β-lactam ring)C═O···H−N−Ala237) result in a catalytically favorable distance (∼3 Å) between the attacking hydroxyl group of Ser70 and the β-lactam ring.

The MD simulations of the benzylpenicillin-TEM1 complex furnished insights into possible pathways for proton abstraction from the Ser70 hydroxyl group. In agreement with earlier pK_a calculations,[16] the Lys73→Glu166 proton transfer leading to an unprotonated Lys73 is energetically disfavored and, therefore, Lys73 is predicted to not be the general base in the acylation process. The mechanistic proposal in which Glu166 accepts a proton from Ser70 via a water molecule is supported by the present calculations since the Glu166-COO^-···H_2O···HO−Ser70 water bridge is highly stable and is properly oriented for the proton transfer to occur. The Ser130 hydroxyl group and the substrate carboxylate group can also play an active kinetic role through a Ser130-OH→$^-$OOC-benzylpenicillin proton transfer followed by a Ser70-OH→$^-$O−Ser130 process. Overall, by taking into account the present results and those of previous experimental and theoretical work, we propose that the Glu166−Wat1 and the Ser130-carboxylate routes constitute competitive pathways for activating the hydroxyl group of Ser70 in the class A β-lactamases.

Acknowledgment. The authors are grateful to the CICyT (Spain) for a generous allocation of computer time at the CESCA and the CIEMAT. Financial support by MCyT (Spain) via grant SAF2001-3526 is also acknowledged. We thank the NIH for partial support of this work via grant GM44974. N.D. thanks to EMBO for her postdoctoral grant (ALTF-371 2001). D.S. acknowledges Fundación Banco Herrero (Spain) for a grant and is much indebted to Professor L. Pueyo (Universidad de Oviedo) for his encouragement and support.

Supporting Information Available: Benzylpenicillin parameters. Table showing the first peak position of $g(r)$ and its integrated value (6 pages, print/PDF). This material is available free of charge via the Internet at http://pubs.acs.org.

JA027704O